SPECTRAL SIGNATURES OF POINT CLOUDS AND APPLICATIONS TO DETECTION OF ALZHEIMER'S DISEASE THROUGH NEUROIMAGING

Jonathan Bates[1], *Dominic Pafundi* [1], *Prabesh Kanel*[2], *Xiuwen Liu*[2], *Washington Mio*[1]

[1]Department of Mathematics, Florida State University, Tallahasse, FL 32306
[2]Department of Computer Science, Florida State University, Tallahasse, FL 32306

ABSTRACT

We introduce a class of spectral shape signatures constructed from symmetric functions on the eigenfunctions of the Laplacian exponentially weighted by their eigenvalues. Such a construction is motivated by problems that arise in the use of the eigenfunctions for shape comparison, such as indeterminacies in the choice of signs and the particular ordering in which the eigenfunctions are presented. The spectral invariants are applied to the analysis of Alzheimer's disease (AD) data collected by the Alzheimer's Disease Neuroimaging Initiative, in particular, to the problem of determining whether the signatures can aid in early detection of AD through morphology and imaging.

Index Terms— Point-cloud Laplacian, spectral signatures, shape analysis, Alzheimer's disease, ADNI.

1. INTRODUCTION

We introduce a sequence of spectral shape signatures derived from the point-cloud Laplacian and investigate their ability to aid in early detection of Alzheimer's disease (AD) through brain imaging. These signatures generalize the heat-kernel signature of [1] to an over-determined family, a characteristic that is desirable in data representation and analysis because it often enhances our ability to learn features that are able to categorize shapes effectively.

The simplest spectral invariants of a shape are the eigenvalues of the Laplacian, also known as shape-DNA [2]. Richer information about the intrinsic geometry of a shape is encoded in the eigenfunctions of the Laplacian, which have been exploited, for example, for shape registration [3, 4] and clustering [5]. The use of eigenvalues and eigenfunctions is appealing because they are robust to pose and articulation, and they lead to a multi-scale representation that progressively captures finer morphological characteristics and thus can also be designed to be very robust to noise.

Although an eigenvalue of the Laplacian can have multiplicity larger than one, this is rare in shapes representing real data because high multiplicities are usually associated with perfect symmetries. Thus, it is common to assume that the eigenvalues are all distinct and the associated normalized eigenfunctions are well-defined up to sign. It is also common to arrange the eigenvalues $0 = \lambda_0 < \lambda_1 < \lambda_2 < \cdots$ in ascending order, and to order the eigenfunctions similarly. The lower modes are of special interest because they capture the large-scale properties of a shape. In shape comparison it is tempting to assume that the ith eigenfunctions naturally correspond. However, counterexamples are known (cf. [3, 4]). Thus, the choice of signs and the correspondence problem suggest that care should be exercised in their use as shape signatures, as already observed by other authors.

To undermine these difficulties, we propose a class of spectral invariants based on symmetric functions of the first k (nontrivial) eigenfunctions of the Laplacian. More specifically, each spectral invariant is a symmetric function of k terms, where each term is a squared eigenfunction weighted by an exponential function of its associated eigenvalue, as suggested by the eigenfunction expansion of the Riemannian heat kernel. We thereby avoid the assumption that the first k eigenfunctions correspond as ordered by the magnitudes of the eigenvalues, and, furthermore, we avoid the sign indeterminacy of each eigenfunction.

The spectral invariants are applied to the problem of early detection of Alzheimer's disease through brain morphology, that is, with the aid of morphological characteristics that may indicate onset of the disorder. Klein *et al.* investigated early stage detection of dementia, considering the morphology of the whole brain [6]. In contrast, we look at the hippocampus, putamen, and thalamus, substructures whose volumes have been noted to change due to neurodegeneration associated with AD [7]. We use magnetic resonance (MR) data collected by the Alzheimer's Disease Neuroimaging Initiative (ADNI) [8, 9]. The aforementioned substructures are segmented with the software *FreeSurfer* [10, 11] from single baseline MR scans of 102 ADNI subjects: 51 normal controls and 51 classified as having mild cognitive impairment (MCI) at the time of the scan and later classified as an AD. MCI is viewed as a precursor to dementia as individuals in this group exhibit an increased risk of conversion. We reiterate that only the baseline scans are used in this study. A statistical summary of the spectral signatures yields a feature

This research was supported in part by NSF grants DMS-0713012 and DBI-1052942.

vector for each subcortical structure of each subject. Then a linear support vector machine (SVM) is trained on these feature vectors. We use the leave-one-out method to evaluate the classification accuracy.

In Section 2 we briefly review the Laplacian and describe the proposed spectral signatures given by symmetric polynomials on the eigenfunctions of the Laplacian weighted by functions of the eigenvalues. In Section 3 we discuss experimental results with various subcortical structures of ADNI subjects. We conclude with a summary and some discussion.

2. SPECTRAL SHAPE SIGNATURES

2.1. Point-Cloud Laplacian

Given a 3D point cloud $P = \{x_i \in \mathbb{R}^3 \,|\, 1 \leqslant i \leqslant n\}$, there are many ways of constructing a graph having P as vertex set and with adjacencies reflecting geometric affinities between them (cf. [12]). We use the ε-neighborhood graph in which two vertices are connected by an edge if the distance between them is less than ε. We employ the measures of affinity

$$w_{ij} = \begin{cases} \exp\left(-\frac{\|x_i - x_j\|^2}{2\sigma^2}\right), & \text{if } \|x_i - x_j\| < \varepsilon\,; \\ 0, & \text{otherwise,} \end{cases} \tag{1}$$

to construct the Laplacian. Let $d_i = \sum_j w_{ij}$ and define the $n \times n$ diagonal matrix $D = \operatorname{diag}(d_1, \ldots, d_n)$. The Laplacian matrix is given by $L = D - W$. We solve the generalized eigenvalue problem $L\phi = \lambda D\phi$ and sort the eigenvalues $\lambda_0, \lambda_1, \ldots, \lambda_n$ in ascending order. We denote the corresponding eigenfunctions $\phi_0, \phi_1, \ldots, \phi_n$. If the graph is connected, λ_0 is the only zero eigenvalue and ϕ_0 is constant. Thus, we focus our attention on ϕ_i, $i \geqslant 1$, especially those associated with the smaller eigenvalues, as they carry information about the global geometry of the point cloud.

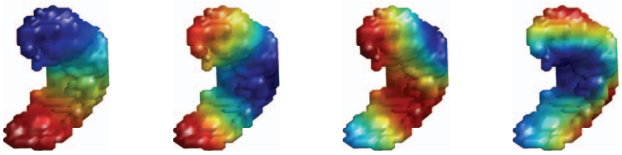

ϕ_1 ϕ_2 ϕ_3 ϕ_4

Fig. 1. Heat maps of the first four nontrivial eigenfunctions of a normal right hippocampus.

2.2. Symmetric Polynomials

By a symmetric function, we mean a function that is invariant under permutations of its arguments. As a preliminary example, consider the symmetric polynomials $f(r,s) = r + s$ and $g(r,s) = rs$ on two variables. An alternative way of constructing these is to fix r and s and consider the quadratic polynomial

$$\begin{aligned}(z - r)(z - s) &= z^2 - (r + s)z + rs \\ &= z^2 - f(r,s)z + g(r,s)\,.\end{aligned} \tag{2}$$

in the variable z. Then, up to sign, $f(r,s)$ and $g(r,s)$ are the coefficients of this quadratic polynomial in z with roots r and s. More generally, for any set $\{r_1, \ldots, r_k\}$ of scalars, we consider the polynomial

$$\prod_{i=1}^{k}(z - r_i) = \sum_{i=0}^{k} a_i z^{k-i} \tag{3}$$

whose roots are $r_1, \ldots, r_k$ and whose coefficients a_i, $0 \leqslant i \leqslant k$, are symmetric polynomial functions on r_i.

2.3. Spectral Signatures

We first truncate the generalized eigenfunctions of the Laplacian at an index k, $1 \leqslant k \leqslant n$ (n being the number of vertices). That is, we only consider $\phi_1, \ldots, \phi_k$. As explained in the Introduction, for each point x in the original point cloud, we will consider symmetric functions on $\phi_i^2(x)$, $1 \leqslant i \leqslant k$, weighted by $e^{-\lambda_i t}$, with $t > 0$. The factor $e^{-\lambda_i t}$ is motivated by the heat kernel on a Riemannian manifold [13], and it allows for the modulation of eigenfunctions associated with higher frequencies and helps to filter out noise. Recall that the heat kernel on a compact Riemannian manifold may be expressed in terms of the eigenvalues and eigenfunctions of the Laplace-Beltrami operator as

$$K(t,x,y) = \sum_{i=0}^{\infty} e^{-\lambda_i t}\phi_i(x)\phi_i(y)\,, \tag{4}$$

where x and y are arbitrary points on the manifold and t may be interpreted as a time parameter. Thus, $e^{-\lambda_i t}\phi_i^2(x)$ is precisely the contribution of the ith eigenmode to $K(t,x,x)$.

Writing $r_i(t,x) = e^{-\lambda_i t}\phi_i^2(x)$ and using (3), we obtain coefficients $a_1(t,x), \ldots, a_k(t,x)$ implicitly defined by

$$\prod_{i=1}^{k}(z - r_i(t,x)) = \sum_{i=0}^{k} a_i(t,x) z^{k-i}\,. \tag{5}$$

For each point x in the point cloud and $t > 0$, the coefficients $a_i(t,x), 1 \leq i \leq k$, give k spectral signatures of the shape. By construction, $a_i(t,x)$ depends neither on the sign of the eigenfunctions nor on their particular ordering.

The signature $a_1(t,x)$, which is the coefficient of z^{k-1}, is given by

$$a_1(t,x) = -\sum_{i=1}^{k} r_i(t,x) = -\sum_{i=1}^{k} e^{-\lambda_i t}\phi_i^2(x)\,. \tag{6}$$

Thus, up to an additive constant, $-a_1(t,x)$ is the point-cloud analogue of the truncated heat kernel $K(t,x,x)$, which is precisely the Heat Kernel Signature (HKS) proposed by Sun *et al.* [1]. Of course, we could set $r_i(t,x,y) = e^{-\lambda_i t}\phi_i(x)\phi_i(y)$ in equation (3) and get

$$a_1(t,x,y) = -\sum_{i=1}^{k} e^{-\lambda_i t}\phi_i(x)\phi_i(y)\,. \qquad (7)$$

Then, $-a_1(t,x,y)$ would give the full truncated heat kernel, again up to an additive constant. However, we restrict our discussion to the simpler $r_i(t,x) = e^{-\lambda_i t}\phi_i^2(x)$.

In analogy with [1], we normalize the coefficients to obtain spectral invariants

$$g_i(t,x) = \frac{a_i(t,x)}{\sum_{y\in P} a_i(t,y)/n}\,, \quad 1 \le i \le k\,, \qquad (8)$$

where P is the point cloud and n is the total number of points in P.

3. EXPERIMENTS

We carried out experiments with a total of 102 ADNI (www.loni.ucla.edu/ADNI) subjects representing two different groups: 51 normal controls and 51 subjects classified as MCI at the time of a visit and as AD at a subsequent visit. We refer to these two groups as NL-NL and MCI-AD, respectively. The main goal was to test how effectively the spectral signatures can differentiate these two groups, that is, how well they can help to predict onset of Alzheimer's disease. Thus, we only used the baseline MR scans acquired prior to the development of AD for patients in the MCI-AD group. For each subject, we segmented the right hippocampus, putamen, and thalamus with *FreeSurfer* and used a point-cloud obtained from the vertices of a mesh representing the contour of each of these brain structures.

We selected the values of the parameters ε and σ involved in the point-cloud Laplacian as follows. We computed the mean pairwise distance μ over the full point cloud and set $\varepsilon = 0.5\mu$ and $\sigma^2 = 0.1\mu$. This produced a connected ε-neighborhood graph for all shapes.

Three functions were used to summarize the behavior of the g_1 signature. For each structure, subject, and $t > 0$, we computed the functions $g_1^{\max}(t)$, $g_1^{\min}(t)$, and $g_1^{\text{std}}(t)$ as the maximum, minimum, and standard deviation, respectively, of $g_1(t,x)$ over all points x in the point cloud. Similarly, we constructed three functions for the signatures $g_2(t,x)$. These functions were sampled logarithmically at T time instants, which are then concatenated to form feature vectors of length $3T$ associated with g_1 and g_2. In our experiments, such feature vectors were sampled at $T = 32$ instants for each of the three subcortical structures. We then trained a linear SVM classifier on these features and computed the classification accuracy based on a leave-one-out strategy. The classification accuracy is recorded in Table 1 for experiments with the right hippocampus, right putamen, and right thalamus, as well as with a combination of all three, which is referred to as "everything". The results suggest that the the lower eigenfunctions play a major role in discriminating the two groups through the proposed signatures, as the improvement from increasing the number of eigenfunctions from $k = 32$ to $k = 512$ is less than 10% with all three substructures taken into account.

Structure	Feature	k	Accuracy
right hippocampus	g_1, g_2	32	71.6%
right hippocampus	g_1	128	72.5%
right hippocampus	g_2	128	70.6%
right hippocampus	g_1, g_2	128	69.6%
right hippocampus	g_1	512	76.5%
right hippocampus	g_2	512	75.5%
right hippocampus	g_1, g_2	512	75.5%
right putamen	g_1, g_2	32	64.7%
right putamen	g_1, g_2	128	56.9%
right putamen	g_1, g_2	512	60.8%
right thalamus	g_1, g_2	32	64.7%
right thalamus	g_1, g_2	128	60.8%
right thalamus	g_1, g_2	512	56.9%
everything	g_1, g_2	32	71.6%
everything	g_1, g_2	512	77.5%

Table 1. Leave-one-out classification accuracy of linear SVM. Feature g_i is an abbreviation for the concatenation of $g_i^{\max}(t)$, $g_i^{\min}(t)$, and $g_i^{\text{std}}(t)$ over 32 time instants. Feature g_1, g_2 means combination of the g_1 and g_2 features. The number of eigenfunctions used, hence the degree of the polynomial, is given by k.

4. SUMMARY AND DISCUSSION

We proposed a new set of spectral signatures of shape of point clouds that may be viewed as a generalization of the heat-kernel signatures of [1]. The spectral invariants are constructed from the eigenvalues and eigenfunctions of the point-cloud Laplacian and circumvent many of the usual difficulties, such as indeterminacy of signs and correspondences, encountered in using the eigenfunctions of the Laplacian to represent shape. We carried out experiments that illustrate the potential of these signatures to aid in the diagnosis of dementia by comparing their behavior on subcortical structures of ADNI subjects comprising 51 normal controls and 51 MCI patients that converted into AD.

Richer summaries of the behavior of the spectral signa-

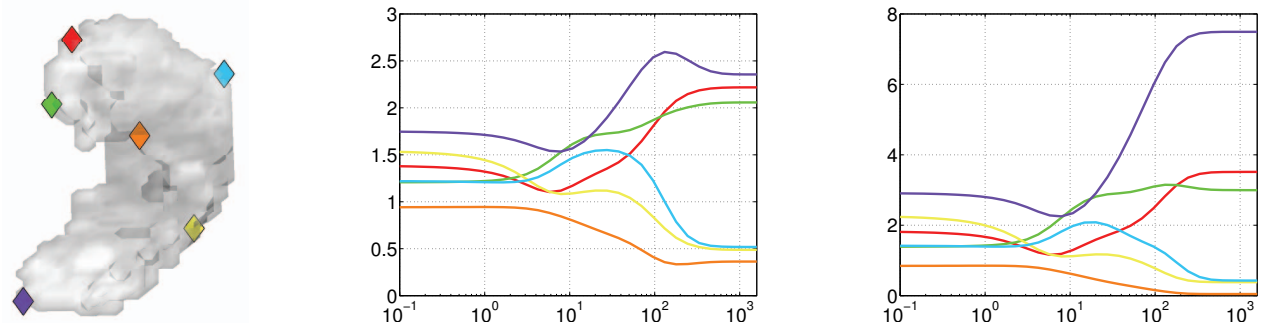

(a) (b) (c)

Fig. 2. (a) A normal right hippocampus with six points marked by colored diamonds; (b) and (c) the g_1 and g_2 invariants, respectively, for these six points are graphed with respect to time t.

tures of a shape remain to be explored. For example, instead of simply looking at their maximum and minimum values, and the spread, one could analyze the full histogram of their distribution over a point cloud, one histogram for each point in time. Other problems to be further investigated are the effect of the choice of Laplacian parameters on the spectral invariants and the use of higher-order spectral invariants. Additionally, various dimension reduction techniques can be applied to the categorization problem via spectral signatures.

5. REFERENCES

[1] J. Sun, M. Ovsjanikov, and L. Guibas, "A concise and provably informative multi-scale signature based on heat diffusion," in *SGP*, 2009, pp. 1383–1392.

[2] Martin Reuter, Franz-Erich Wolter, and Niklas Peinecke, "Laplace-Beltrami spectra as 'shape-DNA' of surfaces and solids," *Computer-Aided Design*, vol. 38, no. 4, pp. 342 – 366, 2006, Symposium on Solid and Physical Modeling 2005.

[3] D. Mateus, F. Cuzzolin, R. Horaud, and E. Boyer, "Articulated shape matching by robust alignment of embedded representations," in *ICCV*, 2007, pp. 1–8.

[4] V. Jain, H. Zhang, and O. van Kaick, "Non-rigid spectral correspondence of triangle meshes," *International J. Shape Modeling*, vol. 13, no. 1, pp. 101–124, 2007.

[5] J. Bates, X. Liu, and W. Mio, "Scale-space spectral representation of shape," in *ICPR*, 2010, pp. 2648–2651.

[6] S. Klein, M. Loog, F. van der Lijn, T. den Heijer, A. Hammers, M. de Bruijne, A. van der Lugt, R.P.W. Duin, M.M.B. Breteler, and W.J. Niessen, "Early diagnosis of dementia based on intersubject whole-brain dissimilarities," in *ISBI*, 2010, pp. 249–252.

[7] L. W. de Jong, K. van der Hiele, I. M. Veer, J. J. Houwing, R. G. J. Westendorp, E. L. E. M. Bollen, P. W. de Bruin, H. A. M. Middelkoop, M. A. van Buchem, and J. van der Grond, "Strongly reduced volumes of putamen and thalamus in Alzheimer's disease: an MRI study," *Brain*, vol. 131, pp. 3277–3285, 2008.

[8] S.G. Mueller, M.W. Weiner, L.J. Thal, R.C. Petersen, C. Jack, W. Jagust, J.Q. Trojanowski, A. Toga, and L. Beckett, "The Alzheimer's disease neuroimaging initiative," *Clin. North Am.*, vol. 15, pp. 869–877 xi–xii, 2005.

[9] S.G. Mueller, M.W. Weiner, L.J. Thal, R.C. Petersen, C. Jack, W. Jagust, J.Q. Trojanowski, A. Toga, and L. Beckett, "Ways toward an early diagnosis in Alzheimer's disease: The Alzheimer's Disease Neuroimaging Initiative (ADNI)," *Alzheimer's Dement.*, vol. 1, pp. 55–66, 2005.

[10] B. Fischl, D.H. Salat, A.J.W. van der Kouwe, N. Makris, F. Sgonne, and A.M. Dale, "Sequence-independent segmentation of magnetic resonance images," *NeuroImage*, in press.

[11] B. Fischl, D. Salat, E. Busa, M. Albert, M. Dieterich, C. Haselgrove, A. van der Kouwe, R. Killiany, D. Kennedy, S. Klaveness, A. Montillo, N. Makris, B. Rosen, and A.M. Dale, "Whole brain segmentation. Automated labeling of neuroanatomical structures in the human brain," *Neuron*, vol. 33, no. 3, pp. 341–355, 2002.

[12] M. Belkin and P. Niyogi, "Laplacian eigenmaps for dimensionality reduction and data representation," *Neural Computation*, vol. 15, pp. 1373–1396, 2002.

[13] S. Rosenberg, *The Laplacian on a Riemannian Manifold*, Cambridge University Press, 1997.